Available online at www.sciencedirect.com
SCIENCE DIRECT®
Bioelectrochemistry 62 (2004) 47–56
Bioelectrochemistry
www.elsevier.com/locate/bioelechem

Supra-physiological membrane potential induced conformational changes in K^+ channel conducting system of skeletal muscle fibers

Wei Chen*

Center for Cellular and Molecular Biophysics, Department of Physics, The University of South Florida, 4202 E. Fowler Ave., PHY 114, Tampa, FL 33620, USA

Abstract

The effects of a supra-physiological membrane potential shock on the conducting system of the delayed rectifier K^+ channels in the skeletal muscle fibers of frogs were studied. An improved double Vaseline gap voltage clamp technique was used to deliver stimulation pulses and to measure changes in the channel currents. Our results showed that a single 4 ms, −400 mV pulsed shock can cause a reduction in the K^+ channel conductance and a negative-shift of the channel open-threshold. Following the Boltzmann theory of channel voltage-dependence, we analyzed the shock-induced changes in the channel open-probability by employing both two-state and multi-state models. The results indicate a reduction in the number of channel gating particles after the electric shock, which imply possible conformational changes at domains that gate the channels proteins. This study provides further evidence supporting our hypothesis that high intensity electric fields can cause conformational changes in membrane proteins, most likely in the channel gating system. These structural changes in membrane proteins, and therefore their dysfunctions, may be involved in the mechanisms underlying electrical injury.

Keywords: K^+ channel; Gating system; Conformational changes; Electric injury; Electric field; Cell membrane

1. Introduction

During an accidental electrical shock or a clinical therapy involving high power electric field, the electric field may cause severe damages to skin, muscle and nerve cells. Clinical manifestations of injury include limb dysfunctions, cell edema, necrosis and finally cell death. In the last two decades, electrical injury diagnosis and patient care have been improved, but not significantly. A reason, perhaps, is that the underlying mechanisms of electrical injury remain unclear. A better understanding of the mechanisms underlying electrical injury is essential in electrical trauma management and patient treatment.

One of the possible mechanisms is electroporation [1,2]. When living cells are exposed to an intensive electric field, pore or pore-like structures may be induced in the phospholipid bilayer of the cell membranes. Formation of these electropores in cell membranes significantly increases ion transfer between the cytoplasmic fluid and extracellular medium, resulting in losses of ionic concentration gradients across the cell membranes. The membrane permeability increment also leads to leakage of cellular metabolic substrates such as ATP molecules, which eventually depletes the cell's energy [3–6].

In addition to electroporation in phospholipid bilayer, an intensive electric field may inevitably affect the membrane proteins, especially the voltage-sensitive proteins. The intensive electric field-induced conformational changes in membrane proteins have been suggested as another mechanism involved in electrical injury [7–10]. The pioneering work on the electrical shock-induced damages in membrane proteins was done by Tsong and Teissie [7] on the Na/K ATPase by using erythrocyte cells. After being shocked by an intensive electrical field, concentration of the radioactively labeled, intracellular Na^+ ions of the erythrocyte cells became higher. They attributed this ionic leakage to alterations of the membrane proteins, Na/K ATPase, since the leakage could be eliminated by ouabain, a specific inhibitor for the Na/K ATPase.

Recently, we have improved the double Vaseline-gap voltage-clamp technique to study the effects of an intensive electric field on cell membrane of skeletal muscle fibers [11]. In addition to electroporation on membrane phospholipid bilayer, we found that the membrane proteins, espe-

* Tel.: +1-813-974-5038; fax: +1-813-974-5813.
E-mail address: wchen@chuma1.cas.usf.edu (W. Chen).

1567-5394/$ - see front matter © 2003 Elsevier B.V. All rights reserved.
doi:10.1016/j.bioelechem.2003.10.006

cially the voltage-dependent membrane proteins such as ion channels, may be affected by the electrical shock, resulting in channel's functional reductions such as decreases in the channel conductance and channel ionic selectivity [10]. The possible mechanisms underlying the membrane protein damages may include large current-medicated thermal effects or supra-membrane potential-coupled structural changes, or both. More recently, our studies showed that for an electric shock generating a membrane potential up to − 500 mV, large transmembrane current-mediated thermal effects did not play a significant role in damaging the channel proteins. Consequently, for this field-strength range, supra-membrane potential-induced proteins' conformational changes have been postulated as the major mechanism involved in membrane proteins' electrical damages [12].

It is still unclear which domains of the membrane proteins are most vulnerable to an external electric field resulting in the channels' functional reduction. One of our hypotheses is the channel gating system because it's voltage sensitivities. This speculation is based on the physiological voltage-dependence of the movable charge particles in the S4 domain functioning as the channel gating system. To support this hypothesis, the ideal experimental evidence would come from direct measurements of the channel gating currents affected by an intensive electric shock. However, many published literatures suggest that the majority of the measured channel gating current in skeletal muscles is not attributed to the K channels. That is partially because of the slow kinetics of K^+ channels.

In this paper, we present results of our recent studies of an electric field-induced damages in the channel gating system by estimating possible changes in the limiting number of channel gating charge particles. We re-measured the K^+ channel conductance with great emphasis on the membrane potentials close to the channel open-threshold. The limiting number of channels' gating charge particles was estimated according to Boltzmann theory for the channels' voltage-dependence. The results suggest that the field-induced reductions in the channel conductance may result from a decrease in number of channels' gating particles. Interestingly, these analytical results also predict a negative shift of the channel open-threshold after the electric shock, which is consistent with our experimental results. These results provide strong evidences to support our hypothesis: the protein domains that gating the channels may be vulnerable to the electric shock suffering structural damages.

2. Material and methods

2.1. Skeletal muscle fiber preparation

The protocol published by others [13–16] with some adjustments was used for the preparation of single muscle fibers [11,12]. Briefly, the skeletal twitch muscle, semitendinosus, was separated from English frogs, *Rana temporaria*, or American frogs, *Rana pipiens*. A single fiber was then hand-dissected and mounted in a custom-made chamber, with two clips at the ends for securing the fiber. The whole fiber was electrically isolated into three pools by two Vaseline-gap partitions. The width of the two partitions and the central pool are 100 and 300 μm, respectively. We then stretched the fiber up to the length of a sarcomere of 3 μm to avoid fiber contraction during electrical stimulation.

The fiber segments in the two end pools were treated with a solution of 0.2% saponin for 2 min to permeablize the cell membrane electrically and ionically, and then washed off using internal solution. A voltage clamp (Dagon TEV 200) was connected to the three pools by six agar bridges and three Ag/AgCl pellets. The total resistance of these agars and pellets was less than 1 kΩ. The voltage clamp controlled by a PC was used to deliver both stimulation pulses and shock pulses. Data was sampled by an Axon data acquisition board (AC 1200) and stored in a hard disk for further analysis.

2.2. Solution compositions

The compositions of each solution were as follows (in mM): Relaxing solution: 120, K-glutamate; 1, $MgSO_4$; 0.1 EGTA and 5, PIPES, External solution: 120, NaCl; 4.25, KCl; 2.15 Na_2HPO_4; 0.85, NaH_2PO_4; and 1.8, $CaCl_2$ Internal solution: 45.5, K-glutamate; 20, Tris–Creatine Phosphate; 20, EGTA; 6.8, $MgSO_4$; 5, PIPES; 5, glucose; and 5.5 Na_2ATP.

A 1 μM TTX in the External Solution has been experimentally tested to effectively eliminate most of the Na^+ channel currents even after electric shock. This shows that the blockage of the Na^+ channel is not affected by electric shocks [10].

2.3. Electrical shock and channel functional assessments

We have suggested an improved configuration of the double Vaseline gap voltage clamp to study the electrical field-induced damages in cell membrane of skeletal muscle fibers [10]. Briefly, the two end pools were connected and a positive feedback circuit was designed to compensate for the voltage drops across the series resistance. The advantages of the improved configuration include a more uniform membrane potential-distribution in the central pool and an elimination of a transient over-shock at the rising phase of the shock pulse.

The experimental protocol is similar to that used in our previous study [10]. Cell membranes were held at − 90 mV. Two groups of pulses were used in the experiments. Step clamp pulses were applied as a sequence of 25 ms step pulses ranging from 20 to 110 mV, which depolarized the membrane potential from − 70 to + 20 mV. When the membrane potential was close to the channel open-threshold, which is defined as a potential where the channel currents start to be measurable, the voltage-step of the

stimulation sequence changed to 2 mV. Shock pulses ranged from − 200 to − 500 mV in magnitude. The durations of all shock pulses were 4 ms in order to simulate exposures to a power-line frequency electric field. A 4-ms duration pulse and a half-cycle sinusoid current at commercial (60 Hz) power frequency with the same RMS value have the same energy.

Before electrical shock, the sequence of step clamp pulses was applied to the isolated cell membrane and the evoked channel currents were recorded. Then a 4-ms supra-membrane potential shock pulse was delivered to the cell membrane. The transmembrane current response was monitored during the shock pulse to determine occurrence of membrane electroporation. Following the shock pulse, the fiber was relaxed until the holding current became stable. The same step clamp pulses were then reapplied to the membrane in order to study changes in the channel currents.

The P/N method was used to resolve the channel currents and the electroporation currents from the step clamp pulse- and the shock pulse-induced transmembrane currents, respectively. When measuring channel currents, four ($N=4$) sub-stimulation pre-pulses were employed preceding each stimulation pulse, which also being referred as P/4 method. The duration of these pre-pulses was the same as the subsequent stimulation pulse, while the magnitude is only 1/4 of the stimulation pulse, which makes these sub-pre-pulses far below the channel open threshold. The linear capacitance and leakage currents crossing the cell membrane or through the pathway underneath the Vaseline seals were recorded responding to those four pre-pulses. These linear currents were then scaled up and subtracted from the stimulation pulse-evoked transmembrane currents. The remaining current was the non-linear current, which have been identified as the delayed rectifier K^+ channel current [10]. With the same method but using a group of sub-shock pre-pulses, the shock pulse-induced electroporation currents can be identified. The number of sub-shock, pre-pulses was eight ($N=8$) to reduce the magnitude of each pre-pulses, thereby avoiding an occurrence of pre-pulse-induced electroporation. For example, for a shock pulse of − 400 mV, the magnitude of the sub-shock pulses is − 50 mV, which is far below the membrane electroporation threshold. Again, all sub-shock pulses had 4 ms duration. Details can be found in our previous paper [10,11].

3. Experimental results

3.1. Shock pulse-induced non-linear leakage currents across the cell membrane

In this control group, the external solution contains channel blockers, TTX, TEA [10] to maximally block the Na^+ and the K^+ channels.

In order to electrically shock the membrane, a 4-ms shock pulse with a supra-membrane potential of − 400 mV was applied to the cell membrane by the voltage clamp. The evoked total transmembrane current was simultaneously recorded, as shown in the upper panel of Fig. 1. If the shock pulse is small enough, less than − 250 to − 300 mV, the current response is a transient peak current with an exponential decay to a plateau representing the membrane linear leakage current. In Fig. 1, the current response to a − 400 mV shock pulse shows a monotonously increasing following the transient peak. This monotonous current increase is the shock pulse-induced, non-linear leakage

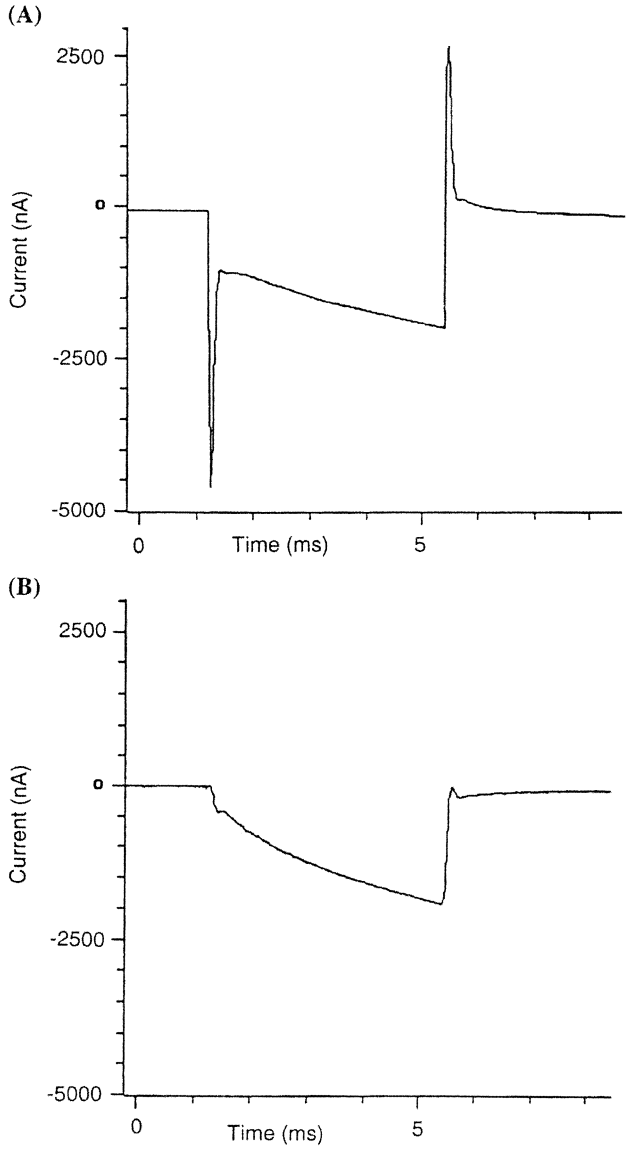

Fig. 1. Transmembrane current recorded during a 4 ms, − 400 mV supra-membrane potential shock-pulse (A). The first transient peak current followed by an exponential-like decay represents the membrane capacitate current. The transmembrane current then increased monotonically until the end of the shock pulse, which is the shock pulse-induced electroporation current (B). Electroporation current was a shock-induced non-linear leakage current, which was obtained by subtracting the linear currents recorded from a group of sub-shock pre-pulses.

currents, which represent either electroporation current or the current resulting from the membrane dielectric breakdown. This electrical shock-induced nonlinear leakage current was explicitly obtained by using the P/N method, and is shown in the lower panel of Fig. 1.

It is necessary to point out that 250–300 mV is only the potential for reversible breakdown of the biological membrane. After the electric shock, the shock-induced transmembrane leakage current can quickly disappear in a time course from milliseconds to seconds. From Fig. 1, after 4 ms, −400 mV pulsed-shock, the increase in leakage currents reduced to zero in a few milliseconds following the fall-phase of the shock pulse.

To confirm the reversibility of the membrane electroporation and the membrane dielectric breakdown induced by a 4 ms, −400 mV, a near-thread pulsed-shock, we performed the following experiments. After the membrane holding current was fully recovered to the pre-shock value, a 30-ms stimulation pulse of −80 mV with four pre-, sub-pulses were applied to the cell membrane. After subtracting the currents responding to the pre-sub-pulses, the currents responding to the stimulation pulse are zero. This result indicates that the membrane electroporation or the membrane dielectric breakdown is fully reversible after a single 4 ms, −400 mV electric shock. The purpose of this control experiment is to rule out the possible contamination of the membrane electroporation to the measurements of channel currents.

3.2. Shock-pulse induced reductions in the K^+ channel conductance, and negative shift of the channel open-threshold

In the following experiments, only TTX was used in the external solution, as described previously. To measure the delayed rectifier K^+ channel currents in cell membranes, a stimulation pulse sequence was applied to the cell by the voltage clamp, consisting of 31 consecutive pulses holding the membrane potentials in a range from −64 to −4 mV. Each stimulation pulse followed four sub-pulses with a magnitude 1/4 of the responding stimulation pulse. The evoked delayed rectifier K^+ channel currents were resolved by P/4 method, and are shown in the upper panel of Fig. 2.

Then, the muscle fiber was shocked by a 4 ms, −400 mV pulse in order to simulate electrical injury. The current response was recorded, which is very similar to those shown in Fig. 1 without visual difference. This similarity indicates that the transient, non-linear leakage currents mainly go through the phospholipid bilayer of the cell membrane.

Following a short period relaxation, the membrane holding currents was recovered to a stable value close to the pre-shock value. Then the same stimulation pulse sequence was applied again to the cell membrane. With the same method, the K^+ channel currents were obtained and are shown in the lower panel of Fig. 2.

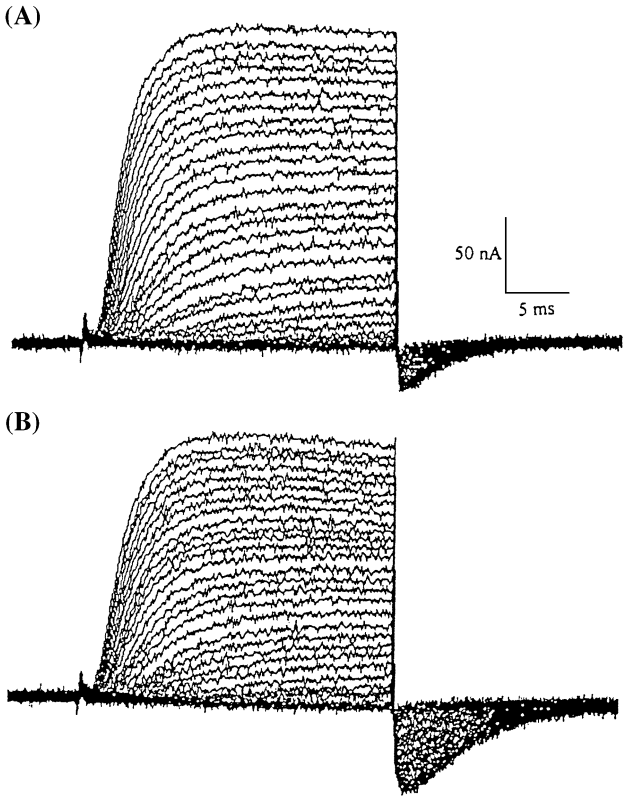

Fig. 2. The delayed rectifier K^+ channel currents recorded immediately before (A) and right after (B) the fiber was shocked by a single, 4 ms, −400 mV supra-membrane potential pulse. The holding potential was −90 mV. A stimulation sequence consisted of 31 consecutive 25-ms depolarized pulses ranging from −64 to −4 mV in steps of 2 mV. Linear capacitance and leakage currents across the cell membrane were subtracted by a P/4 method. The delayed rectifier K^+ channel currents were obtained and shown in the upper panel. The channel current has the highest plateau value corresponding to a stimulation pulse of −4 mV. The consequent channel currents with less plateaus correspond to stimulation pulses of −6, −8... and −64 mV, respectively. After being shocked by 4 ms, −400 mV pulses, the same stimulation sequence was reapplied to the cell membrane. With the same method, the K^+ channel currents were obtained and are shown in the lower panel.

By comparing the pre- and post-shocked channel currents, one can easily notice that the K^+ channel currents responding to almost all of the stimulation pulses were reduced after the electrical shock. The maximum value of the pre-shock K^+ channel currents, about 220 nA, was reduced to around 175 nA, which is an approximately 20% reduction.

The K^+ channel currents in the upper panel are plotted as a function of the membrane potential in Fig. 3, represented by dark circles. The abscissa is the membrane potential held by the stimulation pulses and the ordinate is the evoked channel current. Similarly, the post-shock channel currents from the lower panel of Fig. 2 are plotted in the same figure as open squares. The current–voltage relationship (I–U curve) of the pre-shock K^+ channels differs from the post-shock I–U curve in two aspects. First, the slope of the post-shock I–U curve is lower than that of the pre-shock curve,

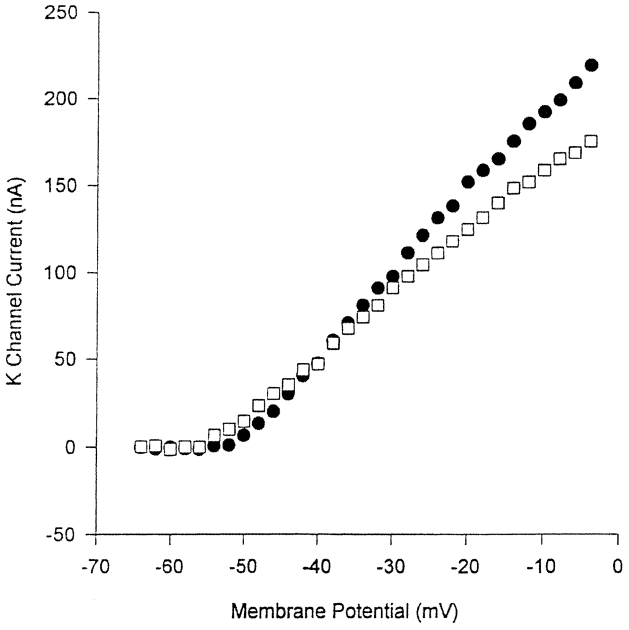

Fig. 3. K^+ channel currents as a function of the membrane potential. The abscissa is the potential to which the membrane was clamped and the ordinate is the evoked channel current. Dark circles and open squares represent the channel currents recorded before and right after the fiber was shocked by a 4 ms, − 400 mV pulse, respectively.

indicating the shock pulse-induced reductions in the K^+ channel conductance. For this fiber, the slope of the curves for the pre- and post-shock K^+ channels, or the channels' slope conductance was 4.4 and 3.5 μS, respectively. A single 4 ms, − 400 mV, pulsed-shock reduced approximately 20% of the channel conductance.

Secondly, the potential threshold where the channel currents start to be measurable is shifted to the negative direction for a few millivolts after the electric shock.

We have noticed that from Fig. 2 the most pre-shock K^+ channel currents are larger than the corresponding post-shock channel currents. But this is not always the case. When small pulses holding the membrane potential slightly positive than the channel potential-threshold, the induced post-shock channel currents were larger than the pre-shock channel currents. This can be seen from the cross section of the two *I–U* curves shown in Fig. 3.

To be clearer, the channel current traces shown in the upper and lower panels of Fig. 2 are redrawn as the left and right panels of Fig. 4, correspondingly. The pre- and post-shock channel current-traces evoked by the same stimulation pulse are placed side-by-side. The numbers in the central column represent the corresponding membrane potentials. Only the membrane potentials ranging from − 64 to − 48 mV are redrawn here. In the left panel, the first trace showing the delayed rectifier K^+ channel currents (out ward current) were not evoked until the stimulation pulse of − 50 mV, while in the right panel, the post-shock channel currents were evoked when the stimulation pulse was only − 54 mV.

This negative shift in the channel critical-potential is also clearly shown in Fig. 3. This result indicates that the single 4 ms, − 400 ms shock pulse may cause a negative shift of the K^+ channel open-threshold.

Nineteen fibers from 13 muscles were studied. All of the fibers showed a shock pulse-induced reduction of the channel conductance, and 12 fibers exhibited a negative shift of the channel potential-threshold. Data will be shown later in Fig. 6.

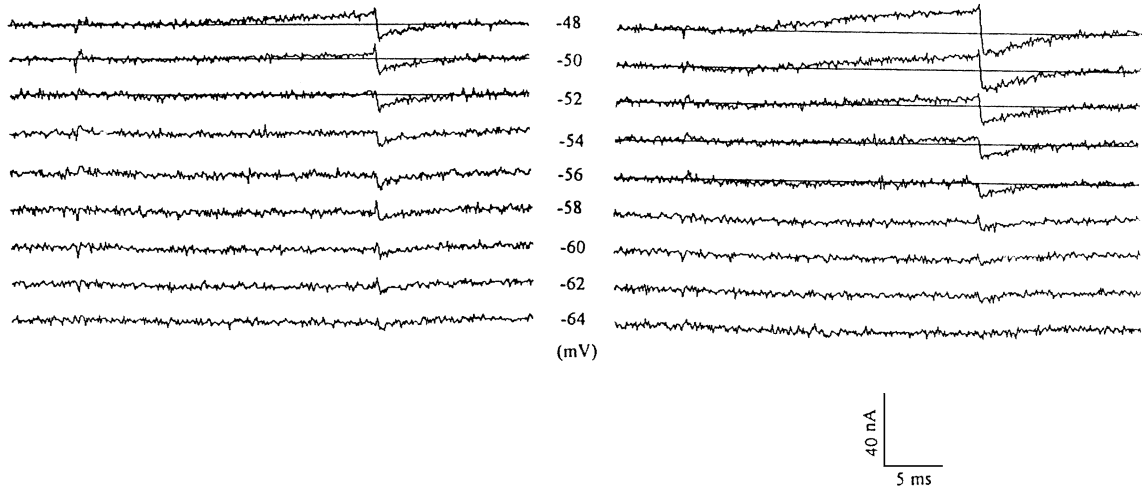

Fig. 4. Redrawn K^+ channel currents shown in Fig. 1. The pre- and post-shock K^+ channel currents evoked by the same stimulation pulse are placed side-by-side in the left and right panels, respectively. Numbers in central column represent the membrane potential of stimulation pulses. The base line currents represent the holding current at a membrane potential of − 90 mV. Only the membrane potential ranging from − 64 to − 48 mV is re-drawn. In the left panel, the first pre-shock channel current was evoked by a step stimulation pulse clamping the membrane potential at − 50 mV; while in the right panel, the first trace shows the post-shock channel current in response to a step potential to − 54 mV.

4. Data analysis

4.1. Estimation of the number of channels gating charge particles affected by an electric shock

4.1.1. Two-state model

Let us first assume a simple two-state model of the K^+ channels: open and closed. According to thermodynamics, the possibilities of channel opening can be described by the Boltzmann distribution of the movable charge particles in the gating system. There are two kinds of energies that dominate the gating charge particles contributed to the open or closed states. One is the protein conformation energy difference between the closed state, E_c, and the open state, E_o. Another is electrical energy, $-zeU$, provided by the external stimulation pulses, where U is membrane potential of stimulation pulses, e is the elementary charge, and z is the number of movable gating charge particles or dipole moments [17,18]. z can also be considered as equivalent valence of the gating charge particle when assuming only one charged particle is mobile among the two-states. The total change in energy from the closed state to the open state responding to the stimulation pulse is $E_o - E_c - zeU$. The ratio of the open state probability, P_o, over the probability of the closed state, P_c, can be described by the Boltzmann equation [18].

$$\frac{P_o}{P_c} = \exp\left(-\frac{E_o - E_c - zeU}{kT}\right) \quad (1)$$

The probability of the open channels among the total number of channels, the relative channel open probability, P, can be obtained by rearranging the above equation,

$$P = \frac{1}{1 + \exp[(E_o - E_c - zeU)/kT]} \quad (2)$$

When the membrane potential is very negative, the first term in the denominator can be ignored because of much smaller than the second terms. By taking the natural logarithm on both sides of the equation, the logarithm of the probability of the open channels can be expressed as a linear equation of the membrane potential U.

$$\ln P = \frac{E_c}{kT} - \frac{E_o}{kT} + \frac{ze}{kT}U \quad (3)$$

From Eq. (3), it is clear that the logarithm of the channel open probabilities, $\ln P$, is a linear function of membrane potential, U, with an intersection, $(E_c - E_o)/kT$, and a slop of ze/kT, which is a function of the number of charge particle, z. Therefore, the number of charge particle, z, can be resolved from the slope of the straight line.

The relative channel open probability can be easily expressed as the relative channel conductance, which is equal to the measured channel conductance, normalized to the maximum channel conductance. The maximum channel conductance can be obtained by stimulating the membrane potential at a very positive pulse, such as +30 mV. By normalizing the measured channel conductance shown in Fig. 3 to the maximum channel conductance, we obtained the pre- and post-shock channel relative open probabilities. Using Eq. (3), these relative channel open probabilities of the pre- and post-shock K^+ channels can be plotted as functions of the membrane potentials, as shown in a semi-logarithm coordinate of Fig. 5.

The abscissa is the size of the membrane potential held by stimulation pulses in a linear scale and the ordinate is the relative channel conductance drawn in a natural logarithm scale. Dark circles and open squares represent the probability of open channels obtained in the control and after the electric shock, respectively. From Fig. 5, the plateau of the relative channel conductance of the post-shock channels is lower than that of the pre-shock, which reflects the field-induced decrement in the K^+ channel conductance.

To study channel relative open-probabilities before and after an electric shock, the measured channels' conductance should be normalized to the pre- and post-shock maximum channel conductance, respectively. Fig. 6 shows the results from all 19 fibers. Dark circles represent the pre-shock channel conductance normalized to the maximum value recorded at a membrane potential of +30 mV, the same as those shown in Fig. 5. The post-shock channel conductance represented by open squares was normalized to the post-shock maximum value at the +30 mV, which is different from Fig. 5. The purpose of normalizing the channel conductance to the post-shock maximal conductance is to obtain the post-shocked channel open probabilities.

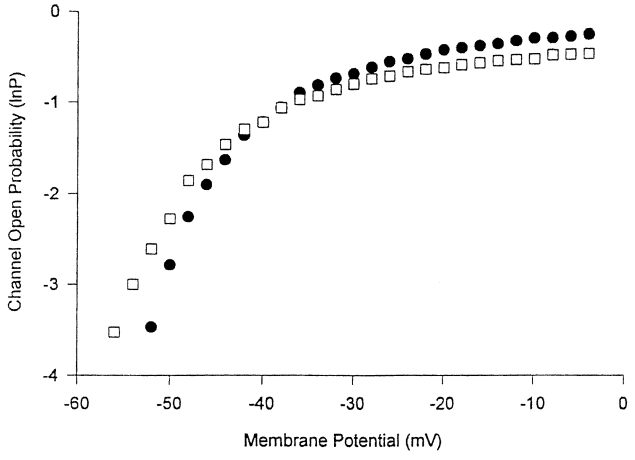

Fig. 5. A semi-logarithm plot of channel open probability expressed as the normalized channel conductance as functions of the membrane potential. X-axis is the magnitude of the membrane potential on a linear scale. Y-axis is the corresponding channel open probability drawn on a logarithmic scale. Dark circles represent control before the electrical shock, while open squares represent the post-shock channel open probability. All channel conductance responding to different stimulation pulses were normalized to the maximum channel conductance, recorded before the electrical shock in response to a stimulation pulse holding the membrane potential at +30 mV, where all K^+ channels are assumed to be open.

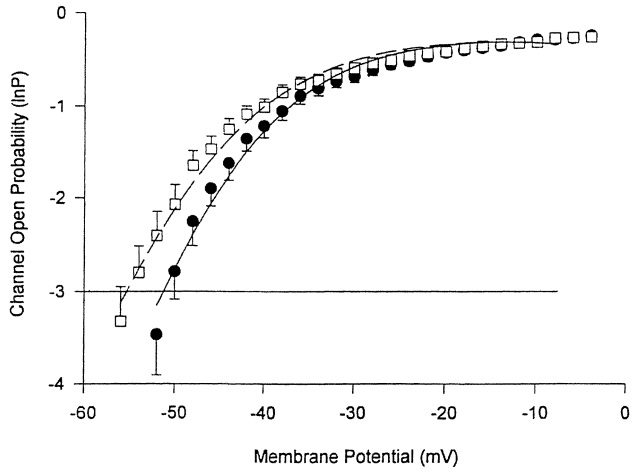

Fig. 6. Channel open probability as a function of membrane potential. The abscissa is the membrane potential in a linear scale. The ordinate is the channel open probability expressed as a normalized channel conductance drawn on a logarithmic scale. Dark circles represent the pre-shock relative channel conductance normalized to the maximum value recorded before the shock in response to a membrane potential of 30 mV. The post-shock channel conductance represented by open squares were normalized to the maximum conductance at the same membrane potential but recorded after the electrical shock. The results were from 19 fibers and the bars are standard errors. Eq. (5) was used to fit the data. The two intersections of the fitted lines with a horizontal line passing through the ordinate of -3 indicate the required membrane potentials to open 5% (e^{-3}) of the channels before and after the electrical shock, respectively. The potential for the post-shock channels is a few millivolts more negative than the pre-shock channels.

It is necessary to point out that when using channel conductance to express the channel permeability, therefore the channel open probability, it implicitly admits an instantaneous current–voltage relation. Indeed, this is not always the case. In general, this is true only when the ionic concentrations crossing the cell membrane are the same and only when one kind of channels exists. However, study from the Goleman–Hodgkin–Katz (GHK) current equation showed that for the voltage-gated Na^+ and K^+ channels, these factors only play a trivial role in the channel conductance steepness [18,19]. The maximum steepness of voltage dependence in the channel conductance is mainly dependent on the channel gating system. In other words, we can attribute the steepness of the K^+ channel I–U curve to the steeply voltage-dependence of channel opening.

Following the assumption we made when we derived Eq. (3), we only focus on very negative membrane potentials which is the rising part of the semi-logarithm plot. From Eq. (3), the rising part of the semi-logarithmic plot can be expressed as a straight line where the slope contains information of the number of limiting charge particles, z, in the channel gating system. The larger the number of the limiting charges particles, the steeper the straight line, or the steeper the rising part of the curve. Fig. 6 shows that the curve slope of the pre-shock channels is steeper than that of the post-shock channels. It indicates that the number of limiting charge particles was reduced by a high intensity electrical shock.

We fitted the rising parts of the two curves to Eq. (3) to two separate straight lines, respectively (not shown). The slope of the best-fit straight line for the pre-shock channels is 4.1 mV per e-fold (2.72) increase of the channel open probability. The value of kT/e is about 24 mV, so that $z = 24/4.1 = 5.8$, which means that the limiting number of charge particles for the pre-shock K^+ channels is about 5.8. The slope of the best-fit line for the post-shock K^+ channels is 5.3, indicating that the limiting number of charge particles in the channel gating system was reduced to 4.5 after the electrical shock. A single 4 ms, -400 mV electric shocks eliminated over 20% of the limiting charge particles in the K^+ channel proteins.

The origin of the ordinate, -4, represents the membrane potential where the K^+ channel open probability is about 2% (e^{-4}). It should be pointed out that the vertical position of the abscissa on the ordinate is randomly chosen. In this study, we chose the origin at 2%, because this is the value closest to the smallest channel currents we can identify. When the origin of the ordinate is chosen at a smaller value, the intersection of the extrapolations of the fitted straight lines with the abscissa will be more negative. This is reasonable because according to the Boltzmann thermodynamic theory, only were membrane potential at negative infinity, all of the channels would be at close state.

When the criterion for the measurable channel currents is defined as the channel open probability of about 5% (e^{-3}), the potential threshold opening the post-shock K^+ channel is 4 mV negative to the threshold for the pre-shock channels. From the intersections of the extrapolations of the straight lines on the abscissa, we see that the difference of the membrane potentials is about 5 mV. A larger membrane potential threshold would be shifted when the criterion of the measurable channel currents is set up at a channel open probability of 2%. In addition, the intersections of the extrapolations of the fitted pre- and post-shock straight lines with the ordinate were also obtained. These two values will be used later in the analysis of multiple-state model.

4.2. Reduction of the limiting number of gating charge particles resulting in a negative shift of the channel open-threshold

4.2.1. Sequential multiple-state model

Our experimental observations include that (1) a lower slope of the post-shock channel open probability drawn as a function of the membrane potential, and (2) a negative shift of the post-shock channel open-threshold.

So far, we only focused on the slope changes by fitting a straight line to estimate the limiting number of charge particles in the channel gating system. The results show that the slope reduction, or the channel conductance reduction, can be well explained by a reduction of the limiting number of gating charge particles. However, the second

observation, or the negative shift of channel open-threshold, has not been considered in our discussion as of yet.

Questions remain. Do these two observations together reveal the same information, a reduction in the channel gating particles? Can a reduction in the channel gating particles explain both two observations? Is the negative shift in channel open-threshold independent of the changes in the slope of the channel open-probability?

To answer these questions, we have tried to fit the data shown in Fig. 6 to Eq. (2) in a whole potential range without the assumption we made in deriving Eq. (3). Unfortunately, the curve did not fit the data well. That is because when using channel conductance to represent the channel permeability and channel open-probability in the two-state model, an instantaneous current–voltage relationship has been assumed. As mentioned previously, we can only attribute the maximum steepness of the K^+ channel I–U curve, obtained at a very negative membrane potential, to the steeply voltage-dependent of channel opening and closing. This assumption is not necessarily true for the whole potential range.

Let us consider a sequential, multiple-state model. In the two-state model, when an external electric field is applied to the cell membrane, the electric energy is only used to overcome the energy difference, $E_o - E_c$, to redistribute the gating charge particles. All these gating charge particles are assumed being free and ready to be relocated. In fact, various chemical bonds in the protein structure may hold the gating charge particles at different close states, so that an extra energy may be needed to free these charge particles. In other words, electric energy has to free the gating charge particles first and then to relocate them. We assumed that the redistribution of the free charge particles from the close state to the open state still followed the Boltzmann distribution, as described above. Charge particles moved from different closed states to the final closed state, where they are ready to move to the open state, can be expressed by a simple first approximation,

$$z = z_0 + nU \tag{4}$$

where z_0 is the free charge particles when the applied external membrane potential is zero and n is a coefficient. In other words, in addition to relocated the free charge particles from closing state to open state (as described in two-state model), the membrane potential also control the number of free charge particles to be moved. Here, the number of free-charge particles, z, is a linear function of the membrane potential, U. By substituting Eq. (4) into Eq. (2), the channel open probability can be expressed as follow:

$$P = \frac{1}{1 + \exp[(E_o - E_c(z_0 + nU)eU)/kT]} \tag{5}$$

We then fitted the channel open probabilities to Eq. (5), shown in Fig. 6, where the value of $(E_o - E_c)/kT$ is the interception obtained in the two-state model previously. The ratio of the best fitted, the number of gating charge particles, z, of the post- and pre-shock K^+ channels at a membrane potential of -50 mV is 0.76. This ratio indicates 24% of the channel gating charge particles was eliminated by the electrical shock, which is relatively consistent with the result of 20% reduction from a two-state model.

More interestingly, the fitted curves clearly show the trends of the relationship between the number of gating charge particles and the channel open threshold. The smaller the number of gating charge particles, not only the more shallow the slope of the curve, but also the more the negative of the channel open threshold. The difference of the membrane potentials is about 5 mV in response to the channel open probability of 5% (e^{-3}), which can be obtained by the intersections of the fitting curves and the horizontal line passing though -3 on the ordinate. These results clearly show that the observations of reduction in channel conductance and negative shift in channel open threshold are necessarily correlated as a result of the decrement in the number of charge particles.

In fact, reductions in the gating charge particles resulting in both a smaller slope of the open probability-curve and a negative-shift of the potential-threshold can be observed from numerical plots of the channel open-probability in terms of various number of the charge particles by Almers and Hille [17,18]. They employed a two-state model and further assumed that $E_o - E_c$ equal to zero; therefore half of the channels are in the closed state when no external electrical field was applied. The numerical plots showed that the smaller the limiting number of gating charge particles, the lower the slope of the open probability is, and the more negative of the channel open threshold. That is equivalent to Eq. (3), when assuming that $E_o - E_c$ is equal to zero and at a negative potential range, the less the number of charge particles, z, the larger the channel open probability is.

5. Discussion and conclusion

5.1. Performing control experiments to clearly identify the channel currents

Great efforts have been put to eliminate or reduce the artificial effects during the experiments in order to identify the electric field-induced effects on the K^+ channel currents.

5.1.1. Effects of membrane electroporation current on channel current measurements

When shock pulse is not much higher than the potential threshold for reversible breakdown of cell membrane, -300 mV, the post-shock transmembrane leakage currents can quickly reduce to, or close to, the pre-shock leakage current. In all of our experiments, the post-shock stimulation pulse sequence was not applied to the fibers until the full recovery of the holding currents.

In addition, in our control experiments using TTX and TEA-chloride to block channel currents, we showed that the post-shock electroporation currents is fully disappeared, as long as the holding current was recovered to the pre-shock value.

In fact, the shock pulse-induced effects on membrane leakage currents are opposite to the effects on the channel currents: shock pulse electroporates cell membrane therefore increases transmembrane leakage currents, while because of electric-coupled structural changes, the pulse decrease the channel currents.

In conclusion, the current traces shown in Fig. 2 are mainly the measured K^+ channel currents. There is no attempt to fully eliminate the electroporation current through the channel proteins. It is safe to say that electroporation currents have no, or very little, effects on the K^+ channel current measurements. In other words, our measured post-shock channel currents remain the characteristics of the K^+ channel currents, such as TEA toxicity and current kinetics.

5.1.2. Polarization of electrode vs. negative shift of the channel-open threshold

Another concern is the possible polarization of the electrodes induced by a high intensity electric shock. In the situation of microelectrode patch-clamp, large currents through the electrode with mega-ohm series resistance may polarize the electrode for a few millivolts, resulting in a shift in holding or command potential. This is not the case in our experiments. In the double Vaseline-gap voltage clamp technique, the total resistance of the electrode is less than 1 kΩ, thousands times less than that of a microelectrode. We have documented that high intensity electric shock-induced polarization in our experimental electrode is far less than 1 mV [11]. This is one of the reasons of this technique superior to a microelectrode patch-clamp to study electric field-induced damages in skeletal muscle fibers.

5.2. Two-state model vs. a simple multi-state model

In this study, a two-state model was used and Hodgkin–Huxley empiricism was followed to derive the number of the channel gating charge particles. In this model, at very negative membrane potentials where most channels are in the closed state, the channel relative open probability can be expressed as a linear function of the membrane proteins in a semi-logarithm scale. Experimental data in a very negative membrane potential range was used to fit the straight line. This method was well established and used to study the number of gating charge particles of the Na^+ and K^+ channels. However, in this model we can only focus on at a very negative potential range. Therefore, this method cannot predict the shift of the channel open-threshold as a function of the number of channel gating charge particles.

Therefore, a simple multiple-states model was further assumed to fit our experimental data in a full membrane potential range. The results clearly indicated that the more the gating charge particles, the steeper the voltage dependence of the channel open probability, and the larger membrane depolarization needed to open the channels. The multiple-state model used in this study may be the simplest multiple-state model, but the results do not lose general conclusion. Indeed, real situations are much more complicated than either two-state or multiple-state models. However, the purpose of this study is to investigate the field-induced changes in susceptibility of the K^+ channel by estimating alteration in the number of channel gating particles. We, here, emphasize a comparison of the pre- and post-shock channels' gating particles using well-studied models, such as two-state, and simple multiple-state models. Neither attempt is to establish a new model to better describe the system, nor to accurately identify the particle numbers. By using theses models, our results can be easily compared with those obtained by other investigators.

5.3. Discussion

We have studied a supra-membrane potential shock-induced functional reduction in the delayed rectifier K^+ channels, including previous results of reduction in the channel conductance [10] and recent results of the negative-shift of the channel open-threshold. However, mechanisms underlying the proteins' damage in the delayed rectifier K^+ channels are not clear. One possibility is a reduction of the size of the narrowest pores in the channel proteins, resulting in a decrease in the channel conductance. However, it is difficult to imagine that when an intensive electrical field generates electropores in the membrane phospholipid bilayer, the channels' narrowest pores could become smaller. In fact, the shock pulse-induced large transmembrane currents might cause local damages around the narrowest pores (few A^0 in diameter) by thermal effects, making the pores even bigger. Tsong and Teissie [7] suggested that an intensive electric field might induce electroporation on the Na/K ATPase, thus increasing the conductance of the membrane proteins.

The reasonable explanation is that the channel conductance reductions may result from conformational changes in the proteins, especially in the channel gating system. This gating system has been considered as protein domains or subgroups of amino acids carrying charged particles or dipoles, which are susceptible to the membrane potential. The field-induced supra-membrane potential exerts a huge electric force on these domains or subgroups, resulting in movement of the charged particles along, or re-orientation of their dipole moments parallel to, the direction of the applied electric field. This supra-membrane potential may even break down some chemical bonds in the protein structure or disable some mobile charged particles or dipole moments. The outcome is a loss of the channel gating capability, therefore, a reduction in the channel conductance.

To better understand the mechanisms of the electrically injured channel proteins, we estimated and compared the number of gating charge particles for pre- and post-shock K^+ channel proteins. We found clear correlations between the decrease in channel conductance and the negative-shift in channel open-threshold. Both respond to a reduction in the number of channel gating particles. This study provides further evidence in supporting our hypothesis that high intensity electric field can cause membrane protein conformational changes. Most likely, the changes occur in the channel gating system because of its voltage-sensitivity. Consequently, the channels' functions are reduced. In closing, these studies indicate that field-induced conformational changes in membrane proteins are one of the mechanisms involved in electrical trauma.

Acknowledgements

This study is supported by a R01 research grant 2GM 50785 from NIH.

References

[1] J.L. Jones, R.E. Jones, G. Balasky, Microlesion formation in myocardial cells by high-intensity electric field stimulation, American Journal of Physiology 253 (1987) H480–H486.
[2] R.C. Lee, M.S. Kolodney, Electrical injury mechanisms: electrical breakdown of cell membrane, Plastic, Reconstructive Surgery 80 (1987) 672–679.
[3] T.Y. Tsong, Electroporation in cell membranes, Biophysical Journal 60 (1991) 297–306.
[4] R.C. Lee, L.P. River, F.S. Pan, J. Li, R.L. Wollmann, Surfactant-induced sealing of electropermeabilized skeletal muscle membrane in vivo, Proceeding of the National Academy Sciences of the United States of America 89 (1992) 4524–4528.
[5] W. Chen, P. Li, R.C. Lee, Efficacy of non-ionic surfactants for sealing electropermeabilized skeletal muscle fibers, Biophysical Journal 61 (2) (1992) 2427.
[6] R.J. O'Neill, L. Tung, Cell-attached patch clamp study of the electropermeabilization of amphibian cardiac cells, Biophysical Journal 59 (1991) 1028–1039.
[7] J. Teissie, T.Y. Tsong, Evidence of voltage-induced channel opening in Na/K ATPase of human erythrocyte membrane, Journal of Membrane Biology 55 (1980) 133–140.
[8] K. Tsuji, E. Neumann, Structural changes in bacteriorhodopsin induced by electric impulses, International Journal of Biological Macromolecules 3 (4) (1981) 231–242.
[9] K. Tsuji, E. Neumann, Electric-field induced *p*K-changes in bacteriorhodopsin, FEBS Letters 128 (1981) 265–268.
[10] W. Chen, R.C. Lee, Altered ion channel conductance and ionic selectivity induced by large imposed membrane potential pulse, Biophysical Journal V67 (1994) 603–612.
[11] W. Chen, R.C. Lee, An improved double Vaseline gap voltage clamp to study electroporated skeletal muscle fibers, Biophysical Journal V66 (1994) 700–709.
[12] W. Chen, Y. Han, Y. Chen, D. Astumian, Electric field-induced functional reductions in the K^+ channels mainly resulted from supramembrane potential-mediated electroconformational changes, Biophysical Journal V75 (1998) 196–206.
[13] B. Hille, D.T. Campbell, An improved Vaseline gap voltage clamp for skeletal muscle fibers, Journal of General Physiology 67 (1976) 265–293.
[14] L. Kovacs, E. Rios, M.F. Schneider, Measurement and modification of free calcium transients in frog skeletal muscle fibers by a metallochromic indicator dye, Journal of Physiology 343 (1983) 161–196.
[15] M. Irving, J. Maylie, N.L. Sizto, W.K. Chandler, Intrinsic optical and passive electrical properties of cut frog twitch fibers, Journal of General Physiology 89 (1987) 1–40.
[16] W. Chen, C.S. Hui, Differential blockage of charge movement components in frog cut twitch fibers by nifedipine, Journal of Physiology 444 (1991) 579–603.
[17] W. Almers, Gating currents and charge movements in excitable membrane, Review Physiology, Biochemistry and Pharmacology 82 (1978) 96–190.
[18] B. Hille, Ionic Channels of Excitable Membranes, Sinauer, Massachusetts, 2001, pp. 54–58.
[19] D.E. Goldman, Potential, impedance, and rectification in membranes, Journal of General Physiology 27 (1943) 37–60.